**Supporting Information:**

# Transparent Ag@Au-Graphene Patterns with Conductive Stability via Inkjet-Printing†

Lihong Li,[a] Meng Gao,[a] Yuzhen Guo,[a] Jiazhen Sun,[a] Yanan Li,[a] Fengyu Li,[a] Yanlin Song*[a] and Yadong Li[b]

a Key Laboratory of Green Printing, Beijing Engineering Research Center of Nanomaterials for Green Printing Technology, Beijing National Laboratory for Molecular Sciences (BNLMS), Institute of Chemistry, Chinese Academy of Sciences (ICCAS) , Beijing 100190, P. R. China. *E-mail: ylsong@iccas.ac.cn
b Department of Chemistry, Tsinghua University, Beijing 100084, China.

## Supplement of experimental section:

**Materials.** Graphite powder (99.998%, 200 mesh), silver nitrate ($AgNO_3$), hydrogen tetrachloroaurate(III) hydrate (99.9%, $HAuCl_4 \cdot xH_2O$), L-ascorbic acid (AC), trisodium citrate dihydrate (TCD), were purchased from Alfa Aecar. Sulfuric acid (>98%), potassium permanganate, hydrogen peroxide ($H_2O_2$, 30 wt%) and sodium borohydride ($NaBH_4$) were purchased from Beijing Chemical Reagents, P.R. China. All chemicals were used as received without further purification.

### Synthesis of graphene oxide (GO) sheets

GO was prepared by a modified Hummer's method. The graphite powder (3g) was added into concentrated $H_2SO_4$ (120 mL). Then $KMnO_4$ (15 g) was added gradually while stirring, and the temperature of the mixture was kept below 20 °C for 2 h using an ice bath. Successively, the mixture was stirred at 38 °C for 2 h and diluted with deionized water (500 mL) to keep the temperature at 50 °C. Additional water (420 mL) and 30% $H_2O_2$ (20 mL) were added, producing a brilliant yellow mixture. The mixture was filtered and washed with a 10% HCl aqueous solution to remove metal ions, which was followed by a deionized water wash to remove the acid. Then as-prepared GO was treated by ultrasonic homogenizer (4710 series, Cole Parmer Instrument Co.) under 200 W for 0.5 h and was passed through a 1.2 μm filter to remove large size of GO. The solid obtained was vacuum dried overnight at room temperature.

### Synthesis of Ag nanoplates (Ag NTPs)

Triangular Ag nanoplates with controlled size and thickness were synthesized by a modified chemical reduction method reported by Mirkin et al[1] and a seeded deposition method developed by Yin [2] and Xia [3] et al. To control the size of Ag NTPs, it is needed to carefully regulate reaction time, reactant concentration, and the rate of the reactant addition. In a typical synthesis of Ag nanoplates (Ag NTPs), 45 μl of $AgNO_3$

(0.1 M), 3 ml of TCD and 100μl of $H_2O_2$ (30 wt%) were dissolved in 50 ml of $H_2O$ under vigorous stirring. 250 μl of ice-cold $NaBH_4$ was injected into the mixture, which turned yellow, black and then blue within a few minutes, and after 30 min the precursor sample was centrifuged and washed with $H_2O$ twice. The collected sample was redispersed in 10 ml of $H_2O$. To this solution was added 1 ml of PVP (5 wt%) and 40μl of ascorbic acid (0.5 M), and then 0.6 ml of $AgNO_3$ slowly under stirring. After that, 300 μl of TCD was added subsequently, and then a mixed solution containing 60 μl of $AgNO_3$ (0.1 M), 900 μl of TCD was also added slowly (5μL/s), for lateral growth of the Ag nanoplates. The reaction was allowed to proceed for one additional hour. The sample was collected by centrifugation and vacuum rotary evaporation.

**Structure calculation:**

The structure calculation has been performed by using first-principles calculations based on the spin-polarized Discrete Fourier Transform (DFT) within the projector augmented-wave method,[4] as implemented in Material Studio.[5] As equilibrium nanoparticles adopt shapes according to the Wulff rule, particles larger than 3 nm are conveniently modeled by extended surfaces.[6] Here, the metals–reduced graphene oxide interface is investigated for the two crystal planes, (111) for metal and (100) for rGO, according to the above experiment results. The surfaces of Ag NTPs-rGO and Ag@Au NTPs-rGO are represented by five Ag atomic layers or five Au atomic layers and three Ag atomic layers, respectively. In order to construct an appropriate supercell for studying Ag NTPs-rGO and Ag@Au NTPs-rGO, the Ag or Ag@Au (111) surface is modeled with a (6×6) surface cell, and the rGO (001) surface is modeled with a (7×7) surface cell (Figure 4c). Repeated slabs (metal (Ag or Ag@Au) and rGO) are separated by at least 15 Å of vacuum. Structural optimization is performed with the two bottom layers constrained to the theoretical bulk positions. The structures are regarded as converged when the largest element of the gradient is lower than 0.03 eV/Å, and the change in energy and atomic coordinates are smaller than $10^{-5}$ eV/atom and $10^{-3}$ Å, respectively. With these choices, the lattice mismatch between Ag and rGO or Ag@Au and rGO is below 1.6%.

**Reference**

[1] R. Jin, Y. Charles Cao, E. Hao, G. S. Metraux, G. C. Schatz, C. A. Mirkin, *Nature*, **2003,** *425*, 487-490.

[2] (a) C. Gao , Z. Lu , Y. Liu , Q. Zhang, M. Chi, Q. Cheng, Y. Yin, *Angew. Chem. Int. Edit.*, **2012,** *51*, 5629-5633; (b) Q. Zhang, Y. Hu, S. Guo, J. Goebl, Y. Yin, *Nano Lett.*, **2010,** *10*, 5037-5042.

[3] J. Zeng, X. Xia, M. Rycenga, P. Henneghan, Q. Li, Y. Xia, *Angew. Chem. Int.*

*Edit.*, **2011,** *50*, 244-249.
[4](a) P. E. Blöchl, *Phys. Rev. B*, **1994,** *50*, 17953-17979; (b) G. Kresse, D. Joubert, *Phys. Rev. B*, **1999,** *59*, 1758-1775.
[5](a) G. Kresse, J. Furthmüller, *Phys. Rev. B*, **1996,** *54*, 11169-11186; (b) G. Kresse, J. Furthmüller, *Comp Mater Sci*, **1996,** *6*, 15-50.
[6] G. Wulf, *Z. Kristallogr.,* **1901,** *34*, 449-530.

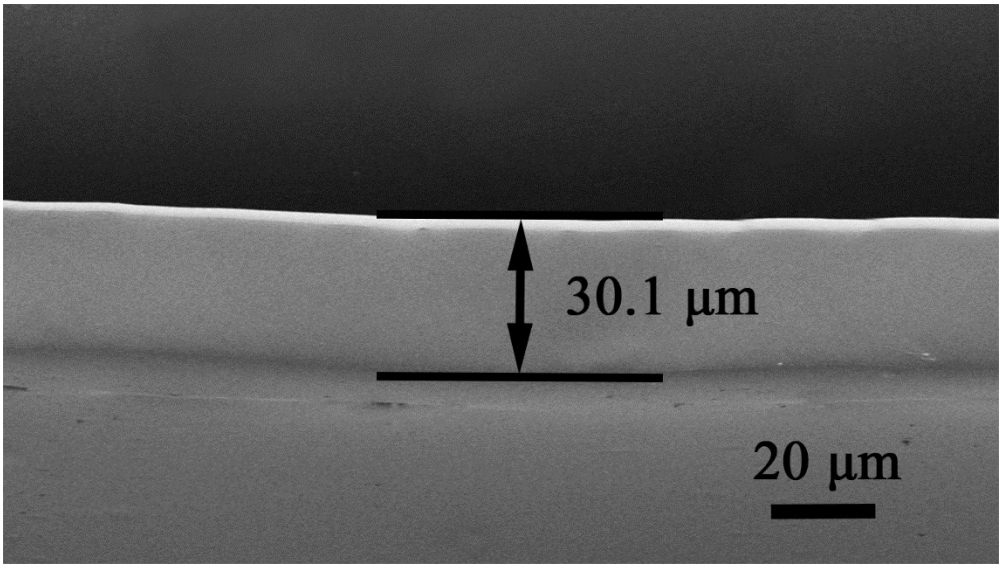


**Fig. S1 The SEM image of the PDMS substrate with thickness of 30 μm, which is formed from the liquid PDMS precursor spin coated on PET film.**

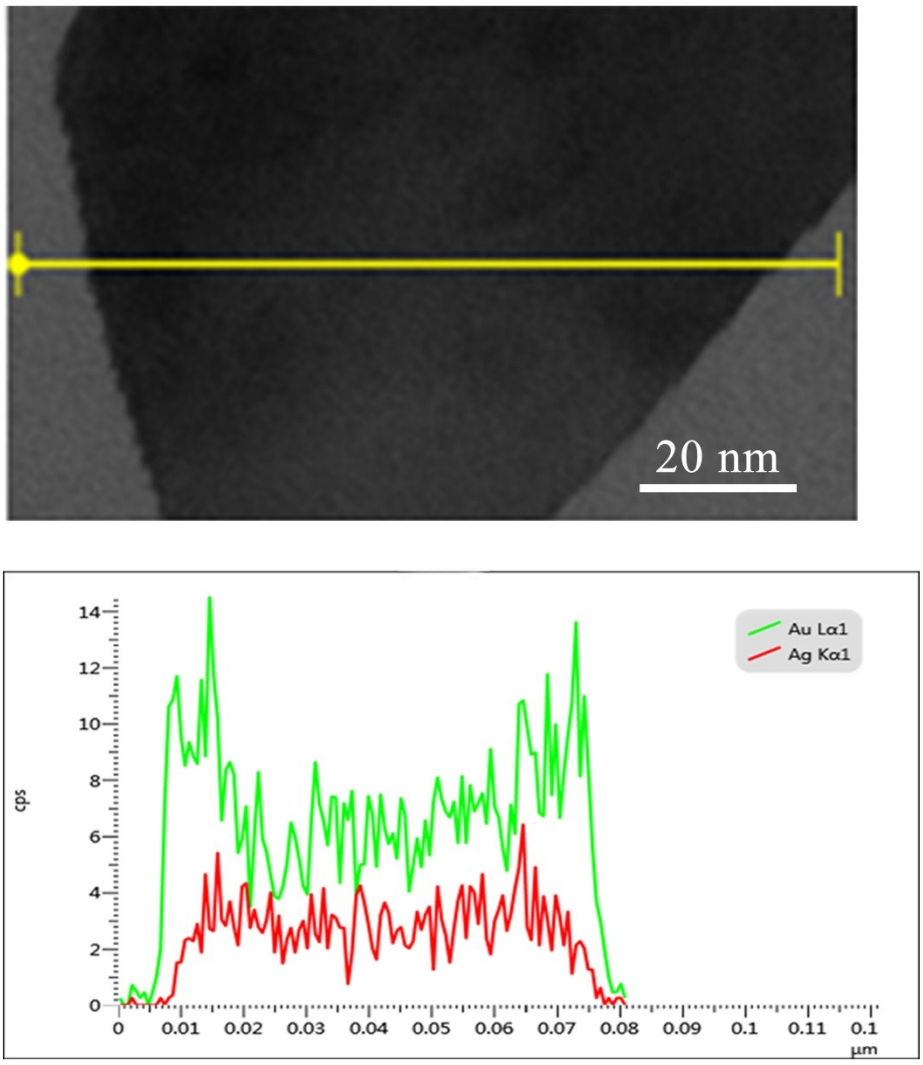


**Fig. S2 The TEM image of Ag@Au NTPs with the corresponding EDS line scan of Ag (red) and Au (green).**

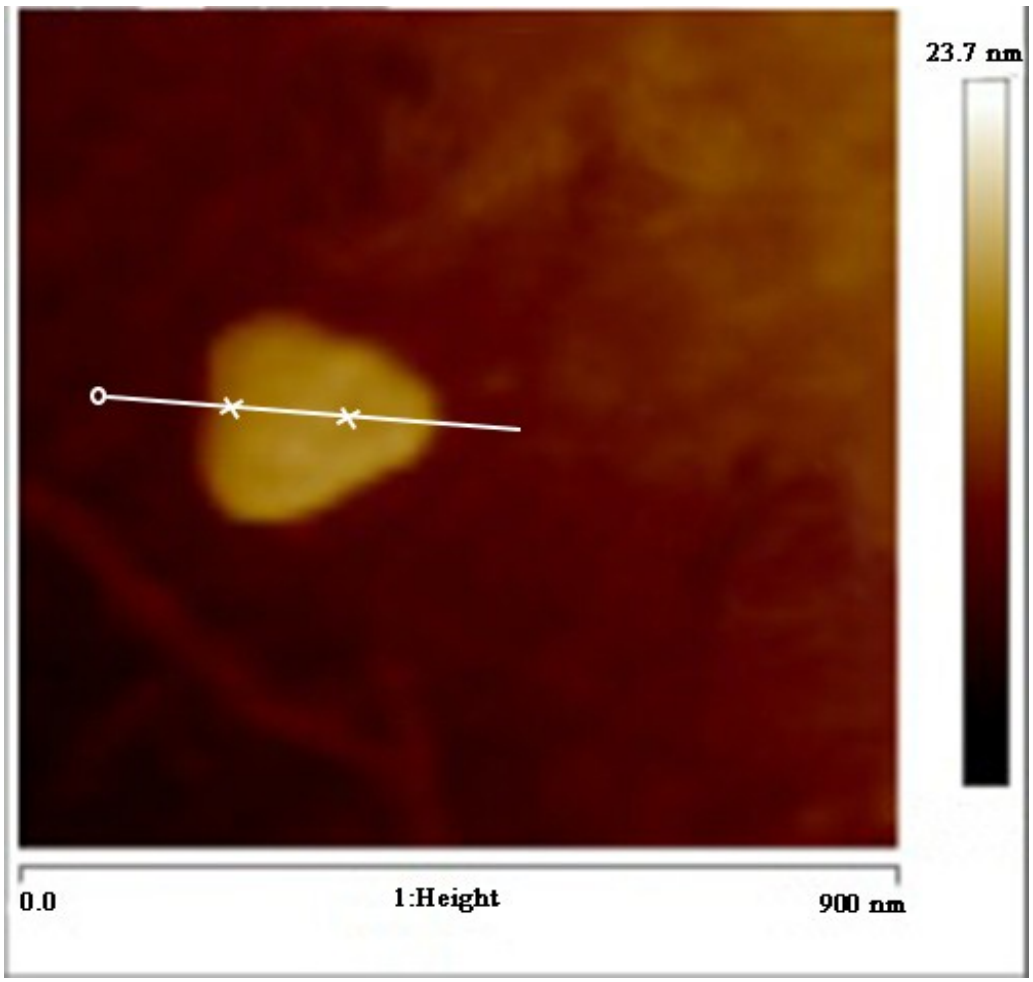


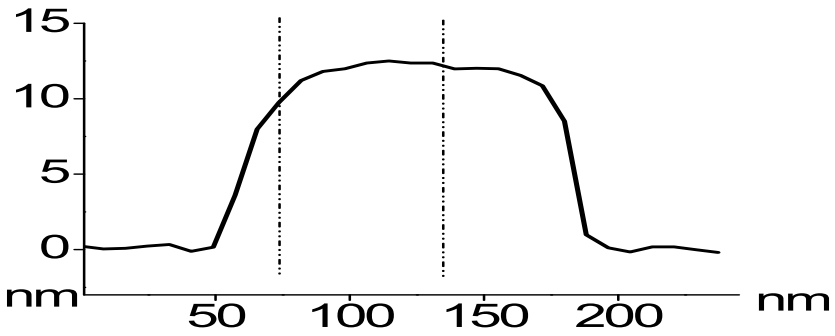


**Fig. S3 AFM image and the thickness profile of Ag@Au NTPs with the well triangle-platelet morphology and a thickness of ~12 nm.**

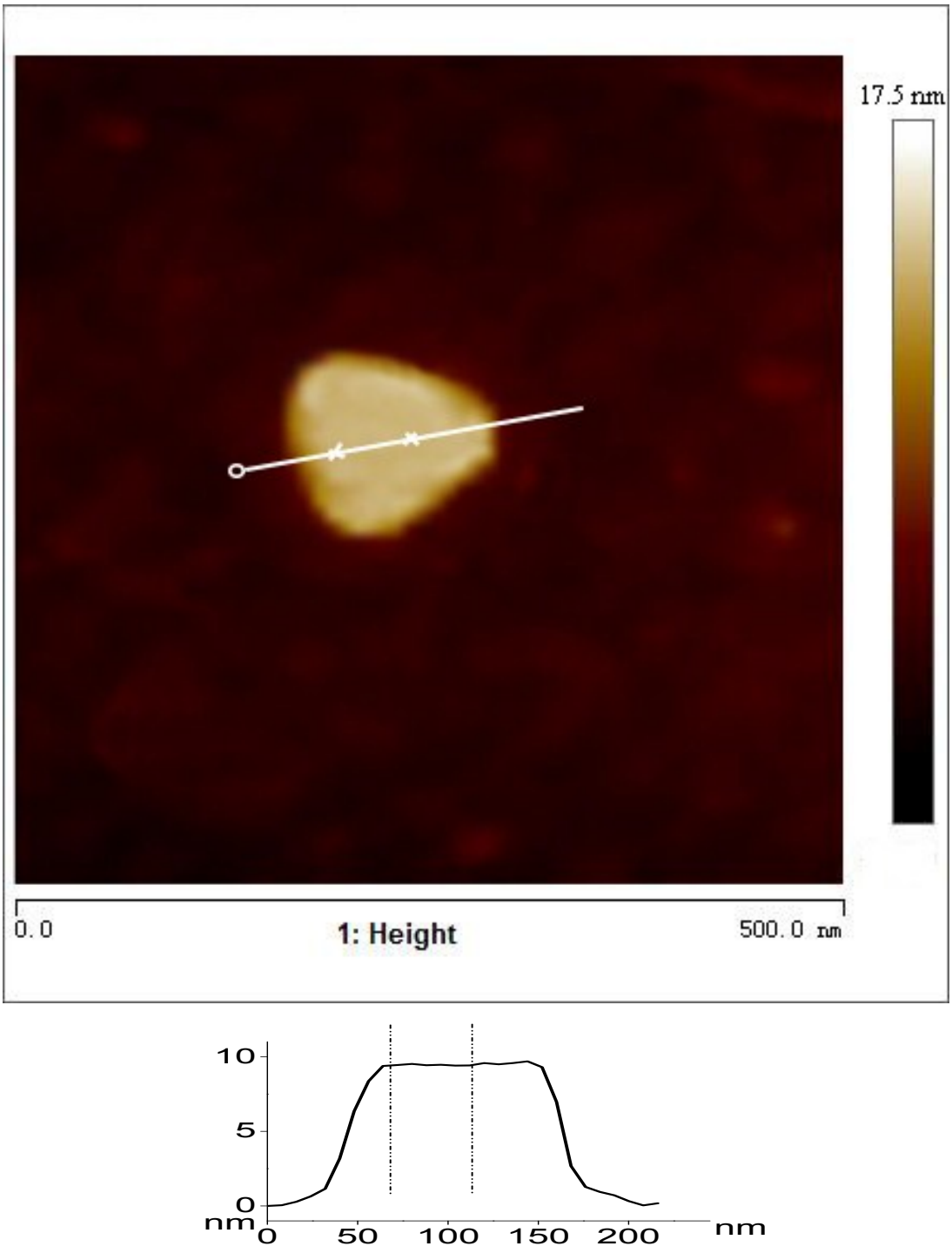


**Fig. S4 AFM image and the thickness profile of Ag NTPs with a thickness of ~9 nm.**

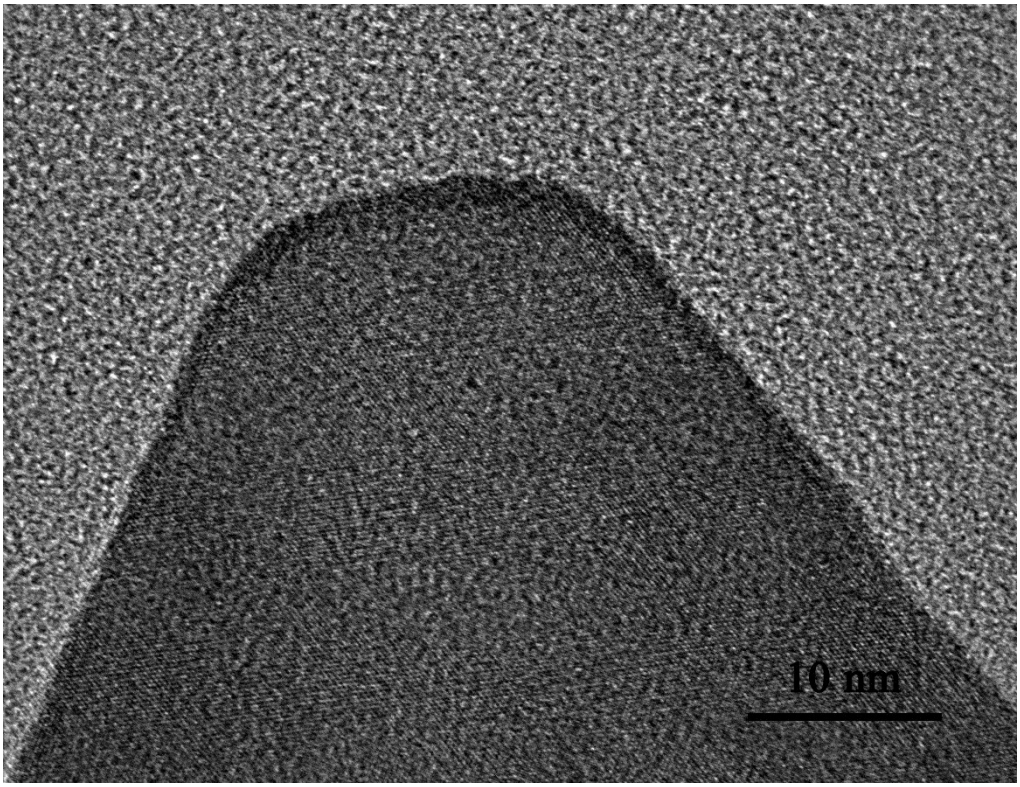


**Fig. S5 The HRTEM image of Ag@Au NTPs, which shows the well crystallinity. A dark line (Au) is around the edge of Ag@Au NTPs.**

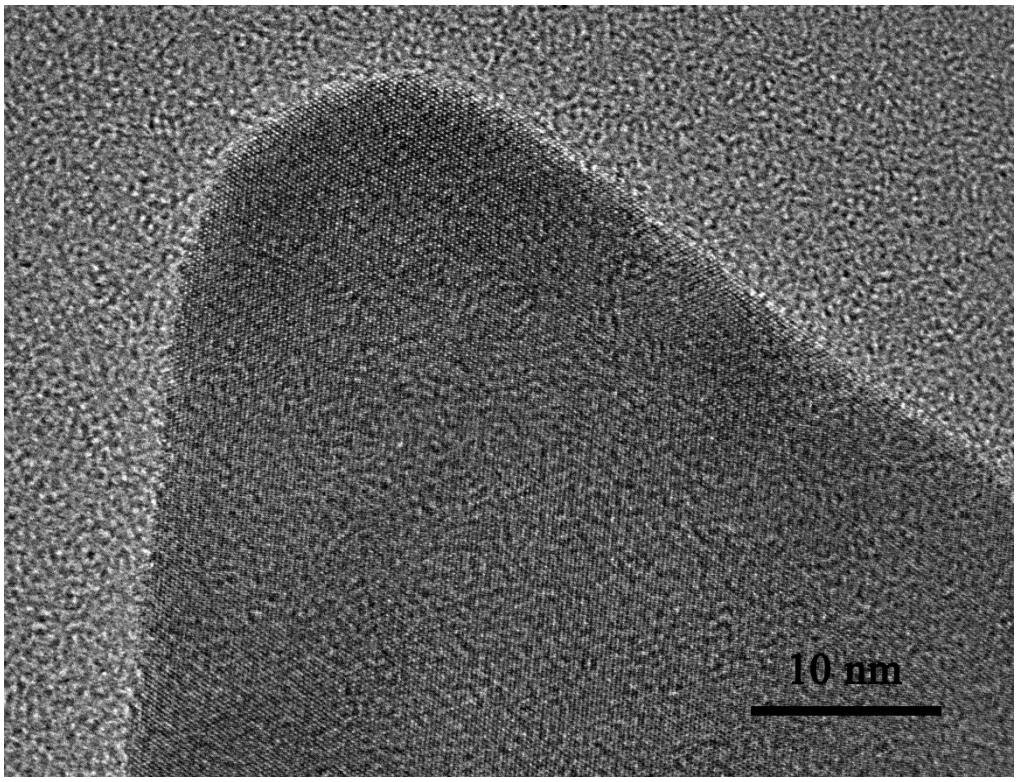


**Fig. S6 The HRTEM image of Ag NTPs, which shows the well crystallinity. No dark line is around the Ag NTPs.**

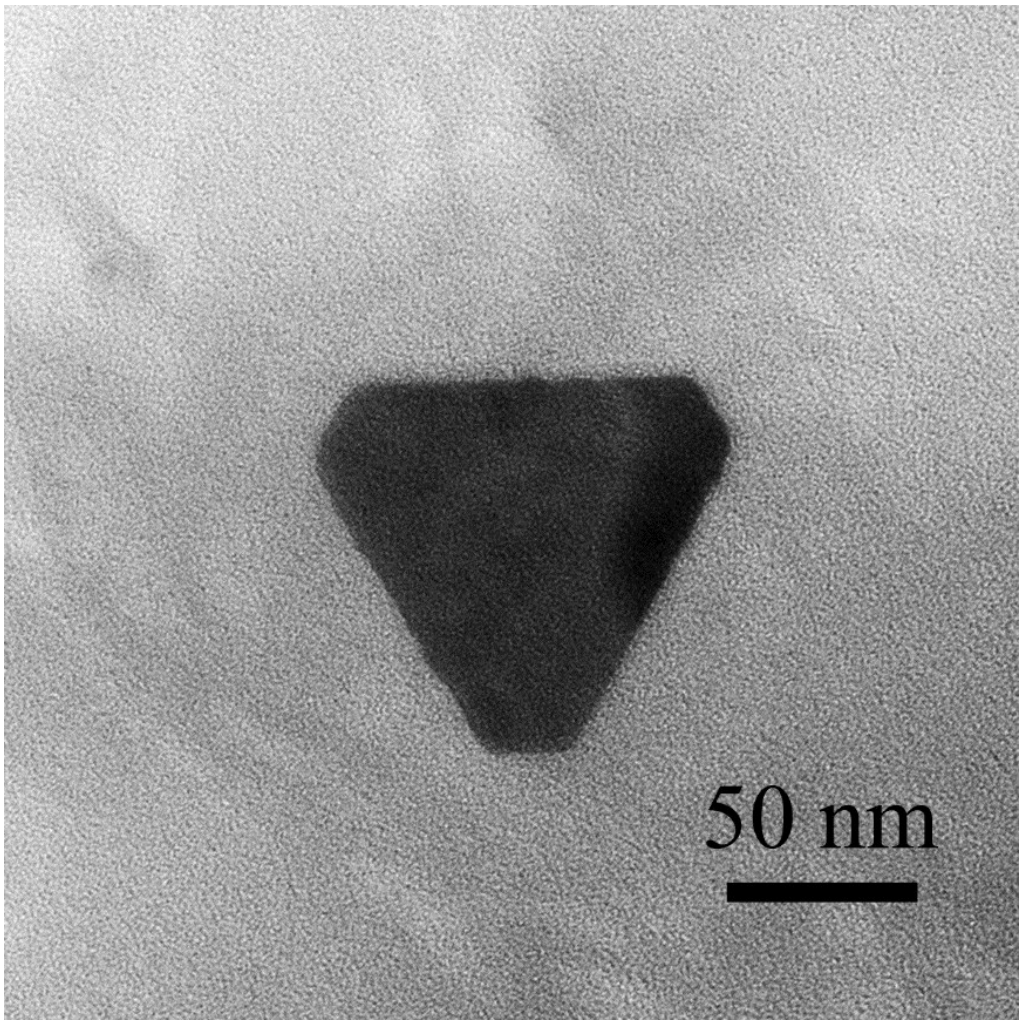


**Fig. S7 The HRTEM images of Ag@Au NTPs-GO.**

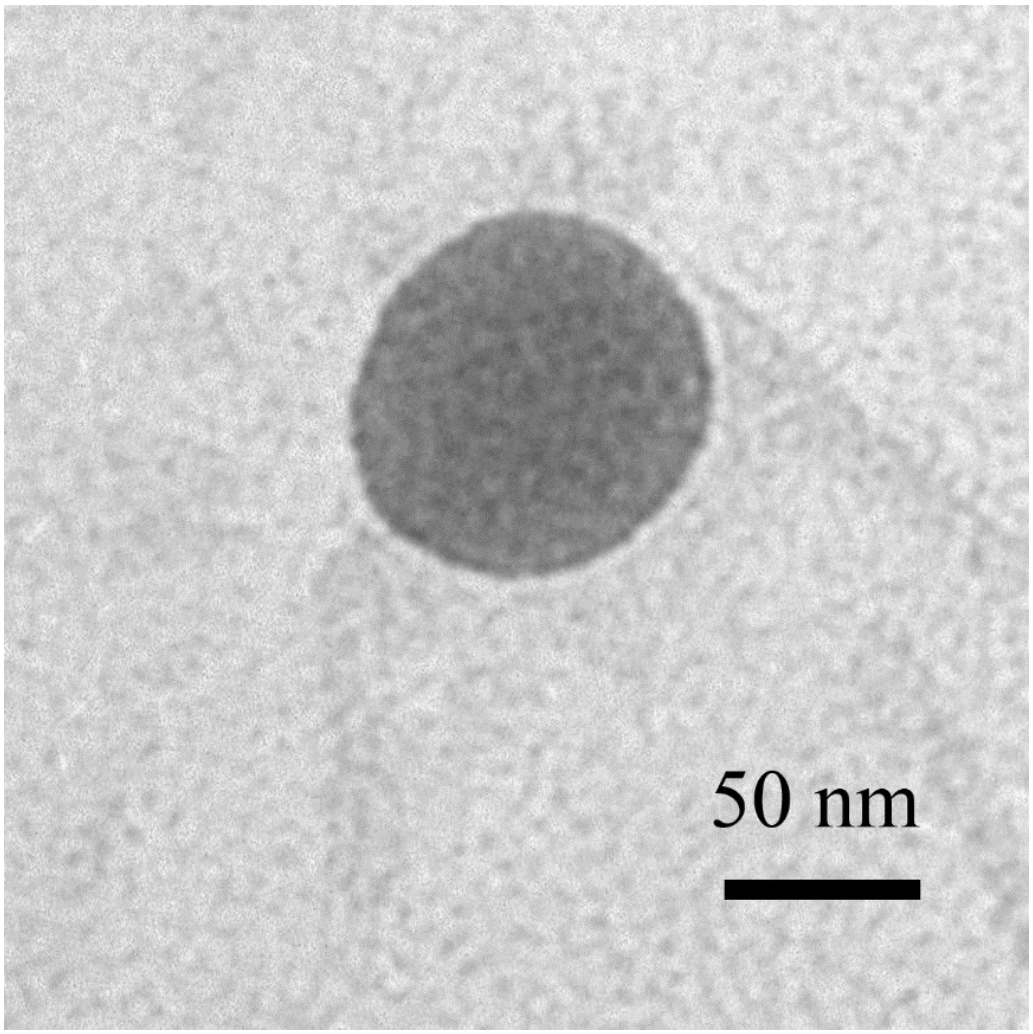


**Fig. S8 The HRTEM images of Ag NTPs-GO.**

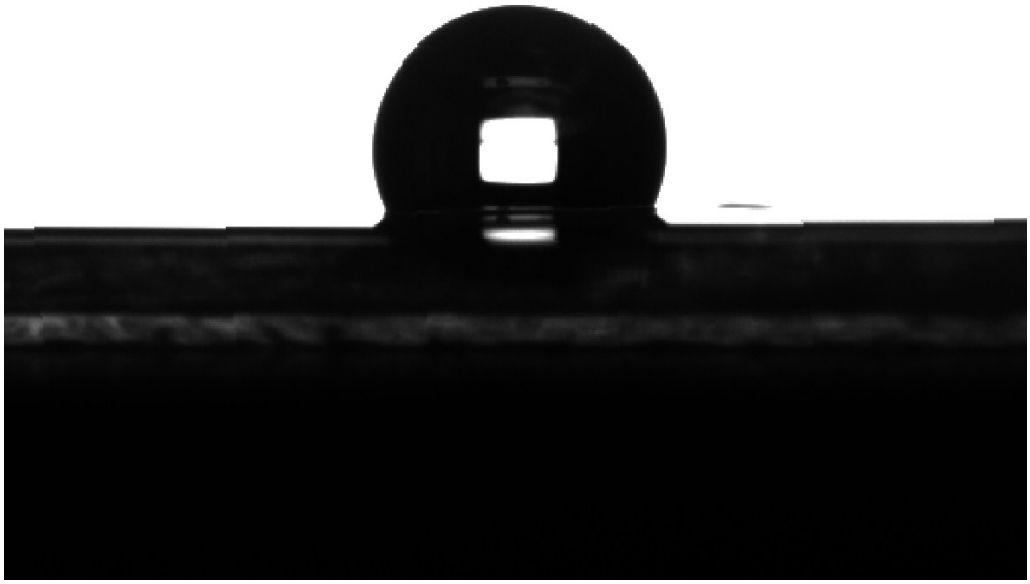

**Fig. S9** the viscoelastic PDMS with the contact angle 121.2$^{o}$.

**Fig. S10** the solid PDMS with the contact angle 102.0$^{o}$.

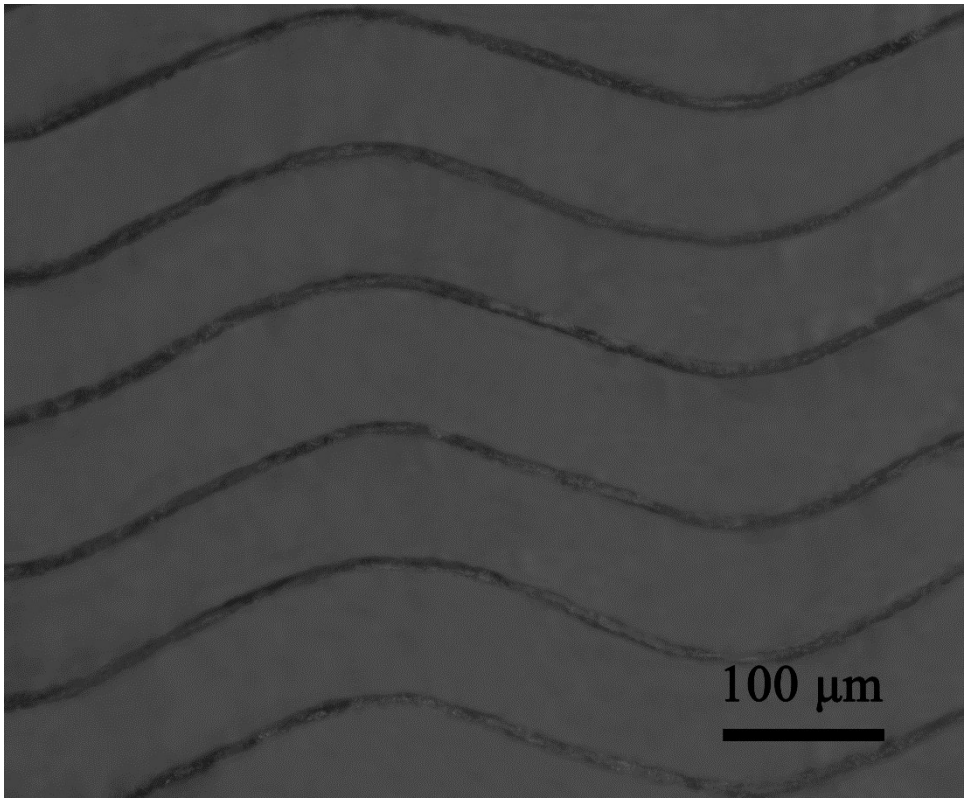


**Fig. S11 The optical microscopy image of the wave patterns inkjet-printed on the viscoelastic PDMS surfaces, which is the favorable patterns for the stretchable devices. The scale bar is 50 μm.**

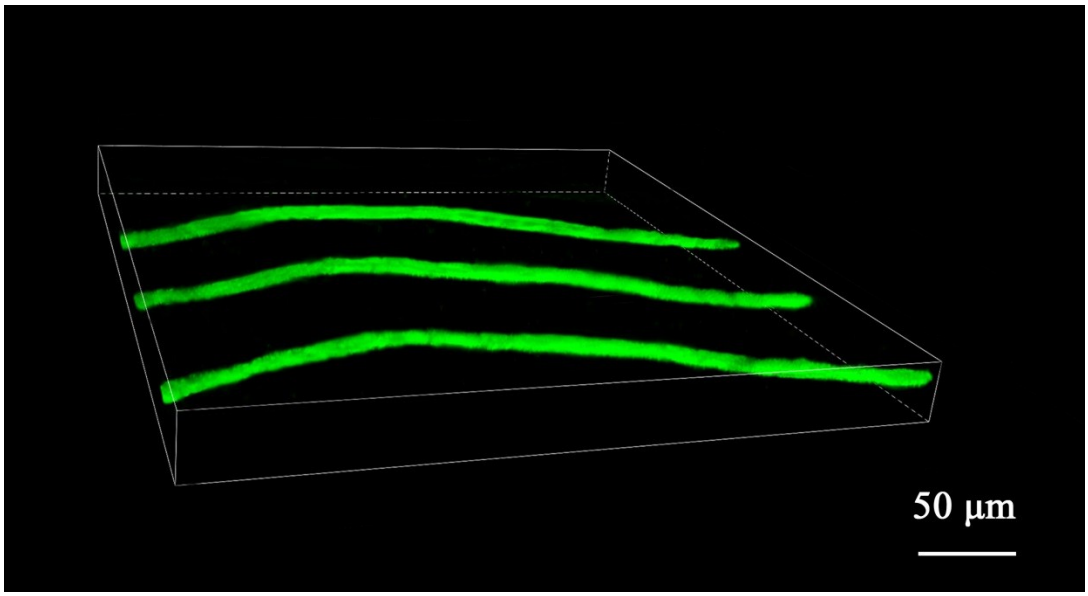


**Fig. S12 The 3D confocal laser scanning microscope image of the wave patterns inkjet-printed on the viscoelastic PDMS surfaces, which is the favorable patterns for the stretchable devices.**

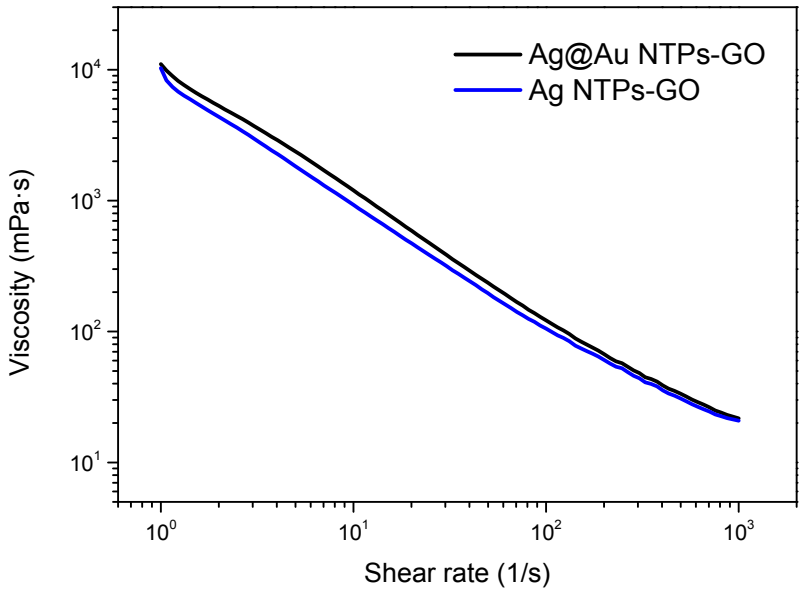


**Fig. S13 Log-log plots of apparent viscosity as a function of shear rate of the Ag@Au NTPs-GO ink and Ag NTPs-GO ink. Both of the Ag@Au NTPs-GO and Ag NTPs-GO inks possess the viscosity that exceeds $10^4$ mPa·s at low shear rates (~1 $s^{-1}$) and exhibit the apparent viscosity of <25 mPa·s at high shear rates (<1000 $s^{-1}$) typically experienced during printing due to the highly shear thinning behavior which allows the ink dropping smoothly through the nozzle during printing.**

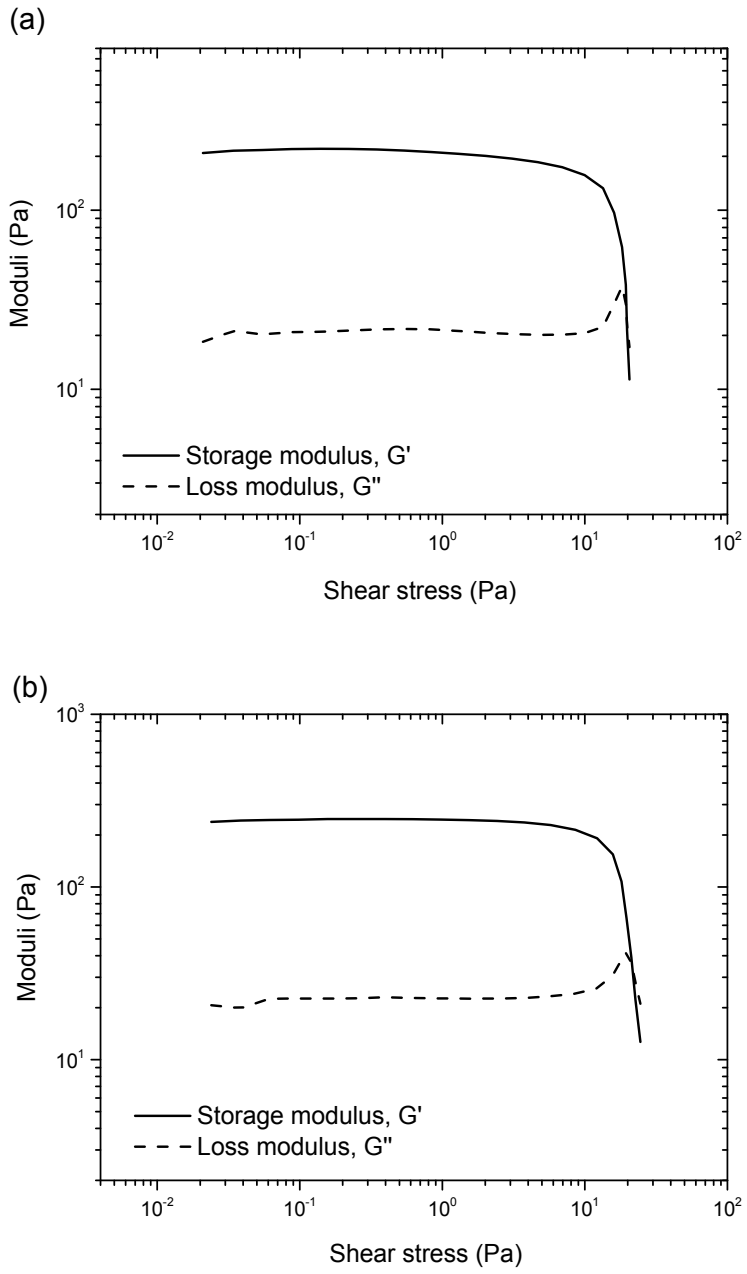


**Fig. S14 Log-log plots of (a) shear storage and loss moduli as a function of shear stress for Ag@Au NTPs-GO ink, and (b) shear storage and loss moduli as a function of shear stress for Ag NTPs-GO ink. The inks exhibit a plateau value of G′~$10^2$ Pa that exceeds G″~10 Pa by about an order of magnitude at low stress (lower than their shear yield stress <10 Pa), therefore the inks can keep their solid-like nature in the quiescent state, and this kind of inks provides the possibility of forming lines on a viscoelastic state surface.**

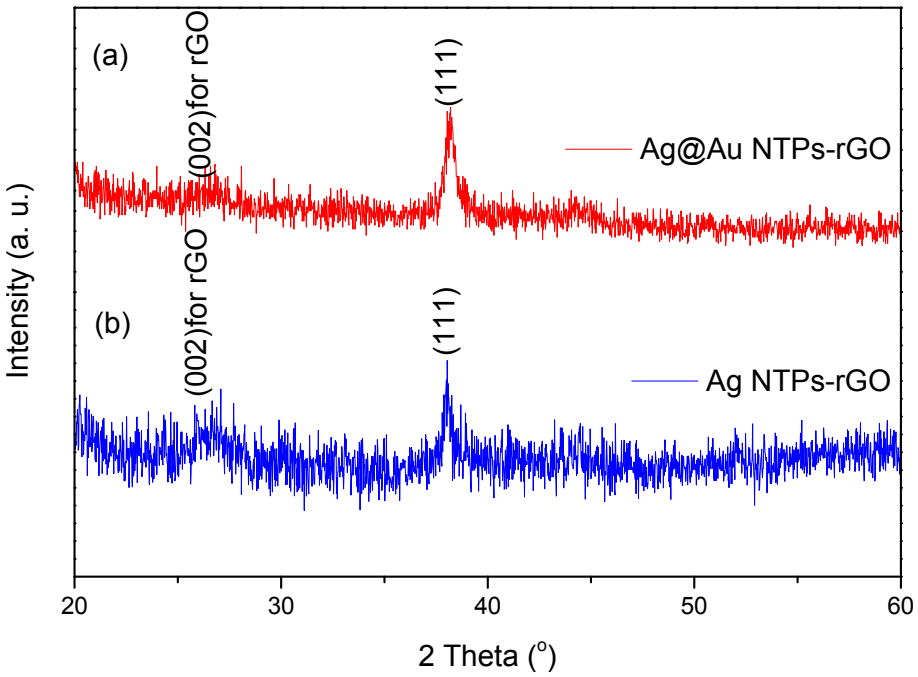


**Fig. S15 The XRD spectra of as-synthesized (a) Ag@Au NTPs-rGO, and (b) Ag NTPs-rGO.**

**Table S1. Analysis of C1s peak positions and the relative percentages of different C species with respect to (a) Ag NTPs-rGO, (b) Ag@Au NTPs-rGO, (c) Ag NPs-rGO100 (100 days later of Ag NTPs-rGO), and (d) Ag@Au NTPs-rGO100 (100 days later of Ag@Au NTPs-rGO).**

| | C-C C=C C-H | C-O | C=O | COOH |
|---|---|---|---|---|
| **Ag NTPs-rGO** | 284.8 (85.4%) | 285.8 (9.7%) | 287.2 (3.1%) | 289.2 (1.8%) |
| **Ag NPs-rGO (100 days later)** | 284.8 (68.6%) | 286 (17.8%) | 287.1 (9.0%) | 288.35 (4.6%) |
| **Ag@Au NTPs-rGO** | 284.8 (88.9%) | 285.7 (7.4%) | 286.8 (3.1%) | 289.07(1.2%) |
| **Ag@Au NTPs-rGO (100 days later)** | 284.8 (87.9%) | 285.7 (7.2%) | 286.8 (3.2%) | 289.1(1.7%) |

**Table S2. The total energies of the interface ($E_{total}$), the energies of the bare metals ($E_{metals,}$ Metals= Ag or Ag@Au), the carbon sheet ($E_{rGO}$), and the interaction energy $E_{interaction}$ of Ag NTPs-rGO and Ag@Au NTPs-rGO are listed.**

| | $E_{interaction}$ (kcal/mol) | $E_{Ag}$ (kcal/mol) | $E_{Ag@Au}$ (kcal/mol) | $E_{rGO}$ (kcal/mol) | $E_{total}$ (kcal/mol) |
|---|---|---|---|---|---|
| **Ag@Au NTPs-rGO** | 87 | | -12894.27 | 1914.87 | -10896.85 |
| **Ag NTPs-rGO** | 24 | -5925.58 | | 1904.86 | -3996.23 |

The total energy of the interface between the metals and reduced graphene oxide sheet is verified according to:

$E_{interaction}=E_{total}-(E_{metals}+E_{rGO})$

Here, the total energies of the interface ($E_{total}$) is compared to the energies of the bare metals ($E_{metals}$, Metals= Ag or Ag@Au) and the carbon sheet ($E_{rGO}$).